ELSEVIER

Contents lists available at ScienceDirect

Chemical Physics Impact

journal homepage: www.sciencedirect.com/journal/chemical-physics-impact



Full Length Article

Synthesis of fluorescent carbon quantum dots from *Manihot esculenta* waste peels for nonlinear optical and biological applications

P. Surendran ^{a,c,1}, A. Lakshmanan ^{b,1}, S. Sakthy Priya ^a, K. Balakrishnan ^c, P. Rameshkumar ^{d,*}, Karthik Kannan ^e, K. Mahalakshmi ^d, V. Gayathri ^d, G. Vinitha ^f

- a PG and Research Department of Physics, Arignar Anna Government Arts College, Affiliated to Periyar University, Namakkal, Tamil Nadu 637 002, India
- ^b Department of Physics, MAM College of Engineering, Siruganur, Tiruchirappalli, Tamil Nadu 621 102, India
- ^c PG and Research Department of Physics, Nehru Memorial College (Autonomous), Affiliated to Bharathidasan University, Puthanampatti, Tamil Nadu 621 007, India
- d PG and Research Department of Physics, Presidency College (Autonomous), Chepauk, Triplicane, Chennai, Tamil Nadu 600 005, India
- e Department of Mechanical Engineering and Advanced Institute of Manufacturing with High-Tech Innovations, National Chung Cheng University, Chiayi County 621301,
- ^f Division of Physics, School of Advanced Sciences, VIT Chennai, Tamil Nadu 600 127, India

ARTICLE INFO

Keywords: Carbon quantum dots Fluorescence Light emitting diode Nonlinear optical Antibacterial activity

ABSTRACT

The synthesis of carbon quantum dots using cassava (*Manihot esculenta*) waste peels by simple hydrothermal method. Carbon quantum dots were studied using PXRD, and HRTEM analysis, signifying an amorphous graphite carbon structure. The carbon quantum dots have two absorption peaks in the UV–vis spectrum, around 272 and 304 nm which lead to the π – π * and n– π * transitions. The produced CQDs exhibit excitation dependent fluorescence characteristics, with a fluorescence quantum yield of 4.664% at an excitation wavelength of 330 nm. The CQDs revealed a white light emitting diode with the Commission Internationale d'Eclairage (CIE) coordinates (0.35, 0.35). The nonlinear optical absorption 0.294×10^{-4} (cm/W), nonlinear refractive index 1.8138×10^{-8} (cm²/W), and third-order NLO susceptibility 5.5×10^{-6} (esu) were calculated using Z-Scan analysis. The synthesized CQDs were utilized for their antibacterial activity used *S. aureus* (23 mm), *B. cereus* (33 mm), *E. coli* (43 mm), and *P. aeruginosa* (30 mm) as harmful microbes. Our results suggest that *Manihot esculenta* waste peels CQDs have potential for application in NLO devices, optical switching, and pharmaceuticals.

1. Introduction

"Carbon" is obviously a very famous term for all and abundantly, which is among the most prevalent elements in the universe. It is commonly found in nature in the form of allotropes, (i.e., diamond, graphite, and amorphous carbon). Recently developed innovative luminescent carbon dots (CDs) have prompted tremendous attention in numerous area's such as bio-imaging, medical treatment, electrocatalysis, and photovoltaic systems owing to their superior ease of processing, low biological toxicity, excellent biocompatibility, and special physico-chemical properties [1,2]. Since the erratic origins of CDs in 2004, numerous methods for the manufacture and production of CDs have been developed to investigate the different characteristics, synthesis processes, and fascinating applications of CDs [3].

In the recent scenario, researchers have been concerned with the

formation of environmentally sustainable green methods for the synthesis of CDs using organic byproducts that consume low-cost raw materials. In the synthesis of CQDs, different methods have been employed, including (i) top-down methods (breaking large carbon materials), like electrochemical exfoliation and laser ablation, or (ii) bottom-up approaches (constructing from smaller precursors), such as microwave and plasma methods, and hydrothermal techniques. Among these, owing to its significant features such as a simple process, the prevention of sophisticated instrumental needs, and the development of strong fluorescence CDs, hydrothermal synthesis has substantially advanced over other current physical approaches [4]. Several byproducts have been used for the synthesis of CQDs, to encourage the manufacture of renewable materials and minimize material waste. Heteroatom (nitrogen, sulfur, phosphorous, florine, and boron) doping is a very effective and easy approach to tuning the optical characteristics and passivating

E-mail address: rameshkumarevr@gmail.com (P. Rameshkumar).

^{*} Corresponding author.

¹ These authors contributed equally as first authors.

the surface of the CDs [5,6]. For example, Adams et al. [7] reported tunable fluorescence CDs as material passivating agents by combustion route carbonization of aqueous starch suspension facilitated by phosphoric and sulfuric acids, respectively [7]. Wang et al. [8] reported cassava starch, a non-food product, which shows potential applications in bio-hydrogen production [8]. Pudza et al., [9] described tapioca-based CDs that are appropriate for sensing and biomedical applications [9]. Reddy Mallem et al. [10] stated that trichromophore doped cassava-based bio-polymers are a hugely exciting luminous component. Device efficiency and excellent reliability underscore the promise of bio-related emission technology using the bio-polymer, cassava, as a platform for the frontier and subsequent generations [10]. Nima et al. [11] synthesized blue-light emitting fluorescent carbon nanospheres with a mean size of 23.6 nm using tapioca via the hydrothermal carbonization process and the luminescent quenching of these performed CNs was strongly selective to the Fe³⁺ ions [11]. In one step, the CDs used to produce the PL chemo-sensor are prepared by mild process conditions from a very inexpensive source of starch (Tapioca sago) were investigated by Basu et al. [12]. Pudza et al. [13] has synthesized CDs which are fantastic fluorescent resources suggested for the adsorption of heavy metal ions [13]. Zhu et al. [14] have investigated a hydrothermal process to prepare N-CDs using ethylenediamine and citric acid as precursors [14]. An organic sustainable hydrothermal reaction of fluorescent N-CQDs with citrus lemon as a source of carbon is stated by Tadesse et al. [15]. Significant attention has been given to increasing the QY and optical performance of CQDs, whereas doping CQDs with other elements, particularly nitrogen, been found to be an appropriate mechanism [16-23].

The objectives of this work were to synthesize fluorescent CQDs with *Manihot esculenta* waste peels and garlic juice extracts using a low-cost hydrothermal method. Various approaches were utilized to investigate the physicochemical properties of CQDs, such as surface functional groups, morphological analysis, elemental analysis, optical properties, and fluorescent studies with quantum yield measurement. In particular, nonlinear optical and antibacterial activities were investigated for optical switching and medical applications.

2. Experimental procedures

2.1. Materials and method

The fresh manioc cassava (*Manihot esculenta*) were collected in the cultivation area and washed several times with double-distilled water. They were then cut into small pieces and placed in a juicer. The juice was then filtered to remove impurities. Finally, fresh *Manihot esculenta* juice (without pulp and without added preservatives) was obtained. Similarly, garlic was bought from the local market and extracted from the juice and ammonia was purchased from E-Merck (99.99%).

Briefly, CQDs were synthesized using 20 mL of Manihot esculenta juice and 2 mL of garlic juice mixed with 8 mL of double distilled water. Followed by the ammonia, which was gradually added to the mixture until pH 7 was reached, the mixture was heated in a Teflon-stainless steel autoclave at a temperature of 200 $^{\circ}\text{C}$ for 6 h After the reaction period, the obtained brown colored solution was further centrifuged at 5000 rpm for 1 h The finally obtained supernatant solution was kept at 5 $^{\circ}\text{C}$ for further analysis.

2.2. Characterization

HRTEM images were captured at 200 kV using a JEOL/JEM 2100 transmission electron microscope. X-ray diffraction analyses were carried out on a PANalytical/ X Pert3 Powder XRD instrument with CuK_{α} (1.5404 Å) radiation. X-ray photoelectron spectroscopy (XPS) measurements were measured on a PHI-VERSAPROBE III (XPS) surface analysis. The FTIR spectrum was acquired over the range of 400–4000 cm⁻¹ using a Perkin Elmer spectrometer. As part of the preliminary

characterization, the UV–vis and fluorescence spectra were measured through the SHIMADZU/UV 2600 spectrophotometer and JY Fluorolog-3-11 spectrofluorometer, respectively. Z-scan analysis was used to assess the third-order nonlinear optical properties of CQDs (HOLMARC Z-scan model: HO-ED-LOE-03).

3. Results and discussion

3.1. Morphological and structural characteristics

The morphologically characterization of CQDs was analyzed with HRTEM. The distributions of particles as well as the surface morphology of the synthesized CQDs are observed by HRTEM (Fig. 1a, b). The HRTEM images revealed that the fluorescence CQDs were spherical in shape. Fig. 1(c) displays the particle size distribution of CQDs, which ranges from 3 to 10 nm, with an average diameter was found to be 6.9 ± 0.5 nm.

Fig. 1(d) demonstrates the XRD pattern of CQDs. The pattern indicates a wide diffraction peak centered at 2θ = 23° , which is similar to the (0 0 2) lattice plane and is due to the disordered structure of the CQDs. This finding was identical to the CQDs that were previously reported [24,25].

The FTIR spectrum suggests the presence of –COOH, C = O, C—H, C—N, and C-S functional groups. It is evident from Fig. 2 that, absorbance band position at $3417~\rm cm^{-1}$, is related to the ν (O—H), weak peaks at $2932~\rm cm^{-1}$ and $2853~\rm cm^{-1}$ are related to ν (C—H). The peak is found at about $1635~\rm cm^{-1}$, which is associated with (C = O) and the absorption band is located at $1409~\rm cm^{-1}$, which belongs to bending vibrations (C—N). The peak position of $1023~\rm cm^{-1}$ could be ascribed to the ν (C-S). Consequently, the FTIR findings attribute that the CQDs surfaces were completely hydrophilic and hydroxyl, carbonyl, and amine groups are identified [26,27]. The hydrophilic surface is possibly the cause of the appropriate water dispersibility which increases the antibacterial activity.

XPS was used to determine the elemental composition of the synthesized CQDs. According to Fig. 3(a), N—CQDs are mostly composed of O 1 s (oxygen), C 1 s (Carbon), N 1 s (nitrogen), and S 2p (sulfur). Fig. 3 (b), shows the two strong binding energy bands at 531 and 532 eV, in the documented spectrum at C–OH/C–O–C, and C = O at respective positions. The C 1 s peaks at 284 and 285 eV shown in Fig. 3(c) indicate that carbon typically exists in the form of C = C, and C—N bonds, respectively. Fig. 3(d) displays two binding energy peaks at 398.8 eV (C–N–C) and 397.7 eV (C–N), respectively [28–31].

3.2. Optical characteristics

In electronic configuration, bandgap, and electronic transformation, the photophysical property has a similar significance. The UV–vis absorption spectrum (Fig. 4) shows two absorption peaks observed at 272 nm and 304 nm, which are ascribed to the π – π^* and n– π^* transitions [32]. The inset Fig. 4 shows that pictures of diluted CQDs obtained under visible light and a UV lamp (365 nm) clearly illustrate that the CQDs reveal a sky blue color when the UV lamp is stimulated. The absorption co-efficient (α) is estimated to be 9.548 and refractive index (n₀) found to be 3.1433 at the wavelength of 532 nm, which can be determined by standard relations [33]. It can be used in the Z-scan section to calculate the NLO susceptibility $\chi^{(3)}$ parameter.

The excitation-dependent emission spectra are shown in Fig. 5. Excitation wavelength is increased from 270 to 370 nm, while emission wavelength is increased from 406 to 442 nm, when the excitation was set to 330 nm, the maximum emission intensity of CQDs was found to be 416 nm. Moreover, the figure depicts the excitation dependent fluorescence emission intensity, which is due to the surface of the CQDs with the quantum effect and numerous emission trap sites such as O-containing groups for illustration and the carboxylate group [34,35].

For CQDs, the fluorescence quantum yield (QY) values were obtained

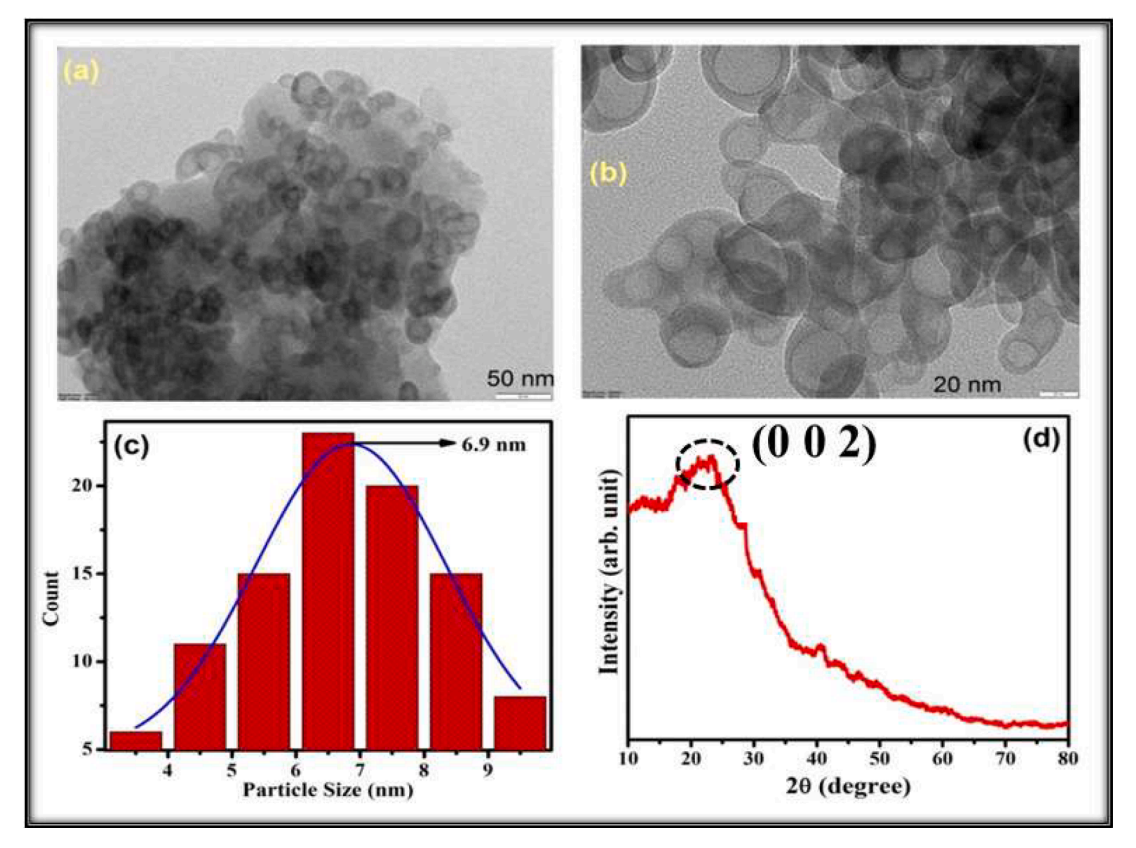


Fig. 1. (a, b) TEM images, (c) corresponding size distribution histogram, and (d) XRD pattern of CQDs.

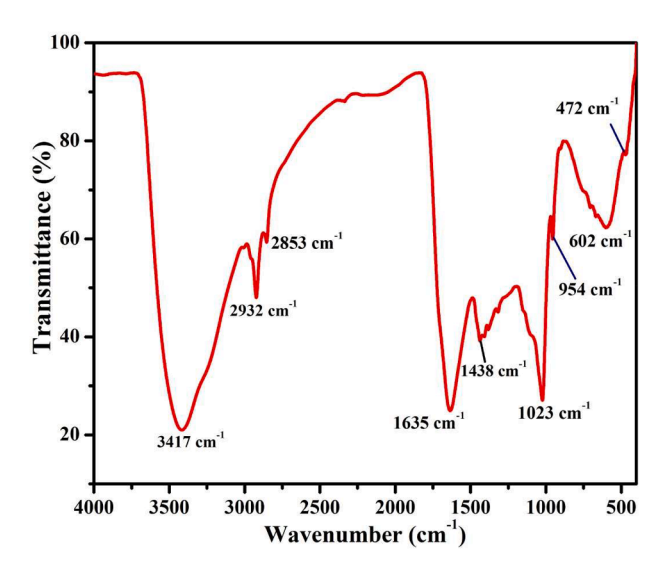


Fig. 2. FTIR spectrum of CQDs.

using an aqueous solution of quinine sulfate (0.1 M) as a standard reference along with the following formulae;

$$QY_x = QY_{std} \times \frac{\eta_x^2}{\eta_{std}^2} \times \frac{I_{std}}{I_x} \times \frac{A_x}{A_{std}}$$
 (1)

where QY represents the quantum yield of the prepared sample (CQDs) and reference sample (quinine sulfate); while " η " describes the solvent refractive index, "I" denote integrated fluorescence intensity, and "A" denotes absorption at 350 nm, the excitation wavelength. The QY was found to be 4.664%.

The CIE created fundamental criteria and measurement techniques

for the lighting industry in order to provide a set of technical requirements for defining and measuring colors. To establish a set of technical standards for defining and measuring colors, CIE developed basic standards and measurement procedures in lighting field. The color coordinate diagram of the CQDs is shown in Fig. 6. The color value is (0.35, 0.35), which is quite near to the value of pure white light (0.33, 0.33). Longshi Rao et al. [36] reported the solvent regulation synthesis of single component white emission CQDs for white LED [36]. G. Ma et al. (2023) has reported Nitrogen-doped carbon dots produced solvothermal using PET waste as a precursor, and their use in LEDs and water sensing [37]. Light-emitting carbon dots derived from naturally growing Torreya grandis seeds were reported by Zhang et al. [38]. CQDs produced with these values can be utilized in white LED applications.

3.3. Z-scan analysis

The third-order nonlinear optical property of the synthesized CQDs was explored by the widely known open and closed aperture Z-scan method. Open aperture Z-scan pattern clearly demonstrates that the CQDs show nonlinear absorption, and valley transmittance at the focus is due to the action of the reverse saturable absorption (RSA). It could be seen that when the sample is shifted away from the point, the normalized transmission first decreases to the target (z=0) and then increases as the material returns to the source. Fig. 7(b) shows the obtained open aperture Z-scan experimental data, whereas the redline fitted theoretically with respect to the equation established by Sheik-Bahae et al. [39].

$$T_{\text{OA}} = \frac{1}{1 + \left(\beta \times L_{\text{eff}} \left\lceil \frac{1_0}{1 + x^2} \right\rceil \right)}$$
 (2)

where β is the absorption coefficient, I_0 is the on-axis irradiance at the focus (Z=0) and $L_{eff}=(1\text{-exp}~(-\alpha L)/\alpha)$ is the effective path length. To find out the nonlinear refractive index of the CQDs, take the difference

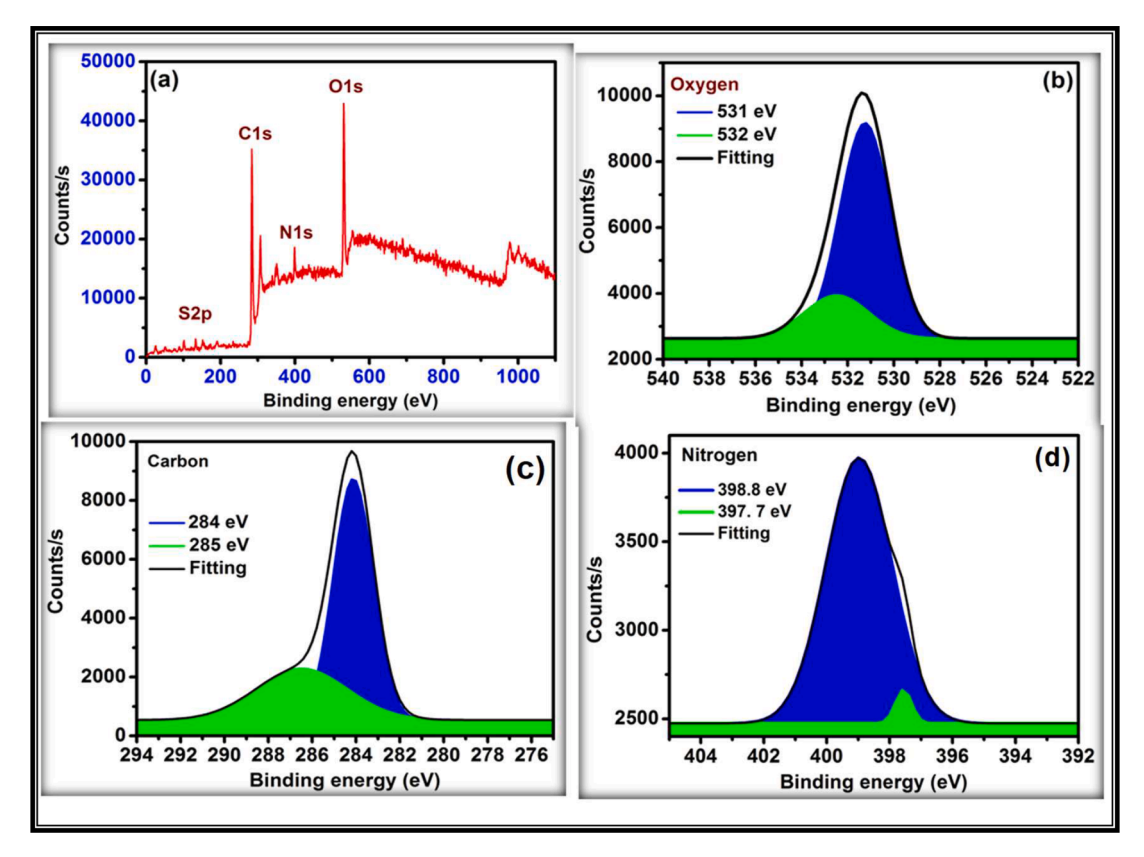


Fig. 3. XPS spectrum of CQDs: (a) XPS survey spectrum, (b) binding energy spectrum of O1s, (c) C1s, and (d) N1s.

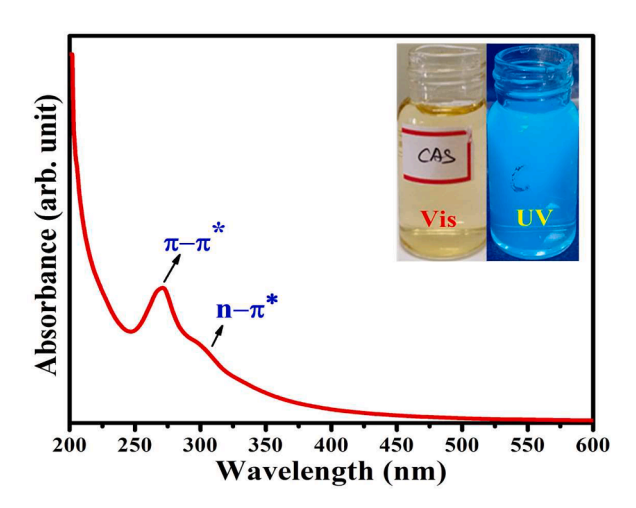


Fig. 4. UV-vis spectrum of synthesized CQDs.

between the normalized transmission peak and valley $(\Delta T_{p\cdot v})$ in the ratio of CA and OA normalized Z-scan patterns as shown in Fig. 7(c). The closed aperture Z-scan method was used to calculate the nonlinear refractive index (n_2) of CQDs. Fig. 7(a) depicts the normalized propagation of CQDs via a closed aperture at a wavelength of 532 nm. Standard relations are used to determine the nonlinear optical properties [40]. The nonlinear optical susceptibility $\chi^{(3)}$ of CQDs can be calculated using the formula,

$$\chi^{(3)} = \sqrt{(Re \,\chi^{(3)})^2 + (Im \,\chi^{(3)})^2}$$
 (3)

The third-order NLO susceptibility of CQDs is calculated as 5.5 \times 10^{-6} (esu). Table 1 summarizes all the estimated values. Table 2 shows that the NLO susceptibility is greater than that of other NLO materials

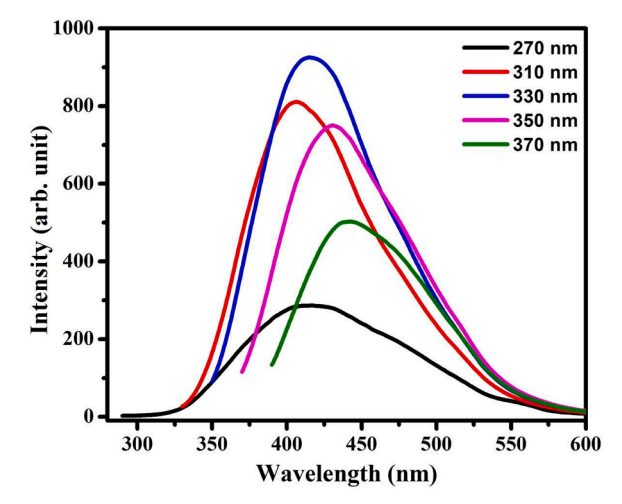


Fig. 5. Fluorescence spectra of synthesized CQDs at different wavelengths.

[41–46]. The comparative data shows that synthesized CQDs have higher NLO susceptibility values, therefore being more suitable for NLO applications. If the CQDs are to be employed in optical switches, the requirements W>1 and T<1 should be fulfilled. The following relationships were used to assess W and T:

$$W = \frac{n_2 I}{\alpha \lambda} \tag{4}$$

$$T = \frac{\beta \lambda}{n_2} \tag{5}$$

The calculated figure of merit value is found to be (W=5.2776) and T=(0.00086232), which perfectly fulfills the condition of suitability for

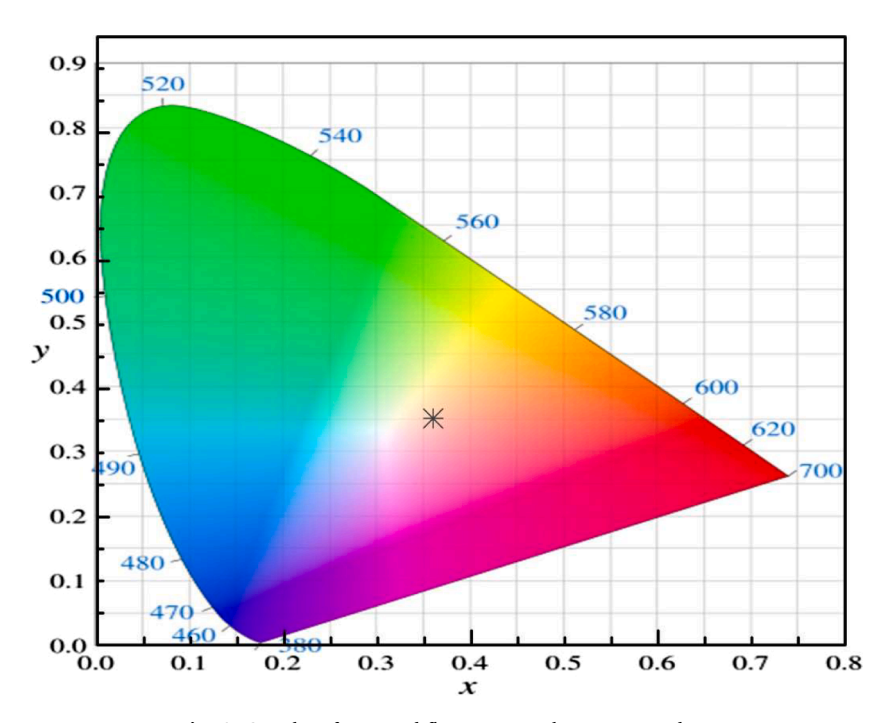


Fig. 6. CIE plot of prepared fluorescent carbon quantum dots.

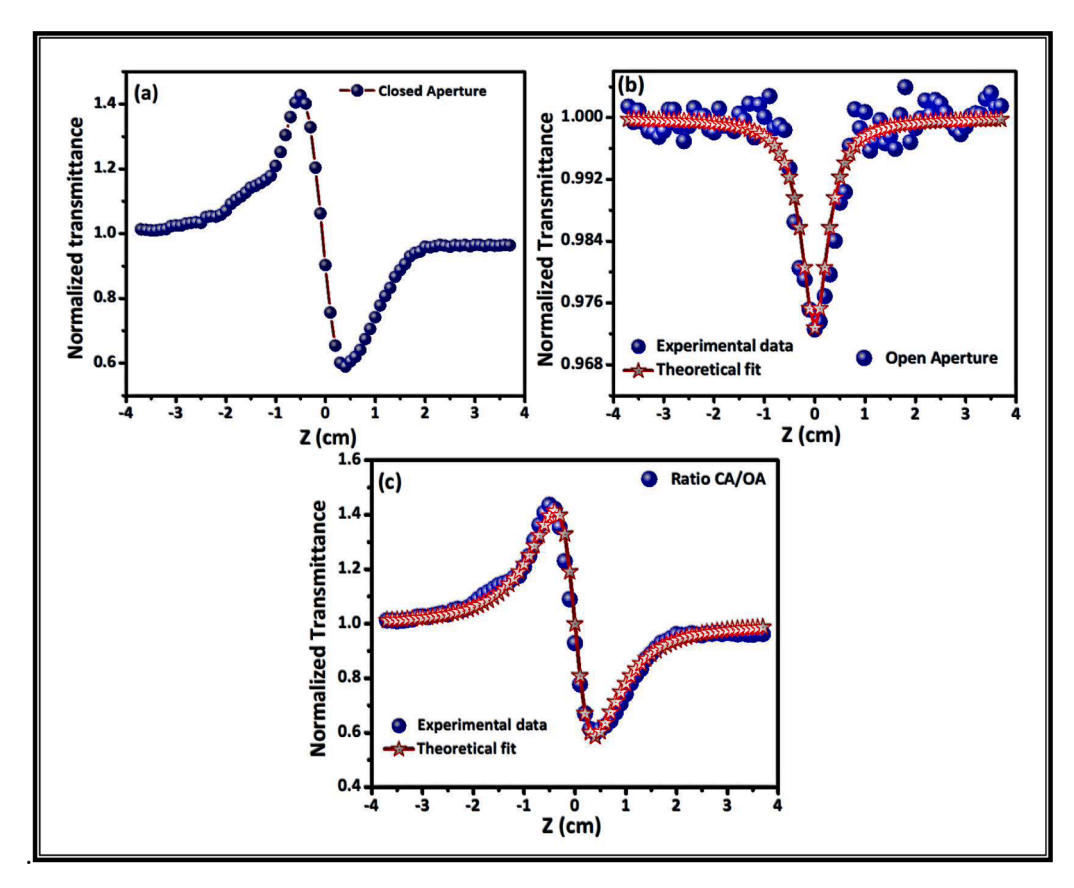


Fig. 7. (a) Closed aperture, (b) Open aperture, and (c) ratio of CA/OA aperture Z-scan pattern of CQDs.

optical switching devices at 532 nm. Because of their reverse saturable properties, the synthesized CQDs are useful for optical switching tools, optical limiters, optical detectors, and sensors for numerous scientific applications.

3.4. Antibacterial activity

The antibacterial activity of the CQDs was tested using Gramnegative (*E. coli, P. aeruginosa*) and Gram-positive (*B. cereus, S. aureus*) microorganisms. Using the disk diffusion technique, clinically isolated

Table 1The nonlinear optical parameters of CQDs.

Parameters	Values
Laser wavelength	532 (nm)
Focal length of lens used	130 (mm)
Radius of aperture used	1.5 (mm)
Radius of the beam on aperture	3 (mm)
Intensity of the laser at the focus	0.01478 (MW/cm ²)
Reighley range (Z _R)	1.271 (mm)
Nonlinear refractive index (n ₂)	$1.8138 \times 10^{-8} (\text{cm}^2/\text{W})$
Nonlinear absorption coefficient (β)	$0.294 \times 10^{-4} (\text{cm/W})$
Real part of NLO susceptibility (Re $\chi^{(3)}$)	4.5388×10^{-6} (esu)
Imaginary part of NLO susceptibility (Im $\chi^{(3)}$)	3.11425×10^{-6} (esu)
Third-order nonlinear susceptibility $(\chi^{(3)})$	$5.5 \times 10^{-6} \text{ (esu)}$

Table 2 provides a comparison of CQDs third-order NLO susceptibility ($\chi^{(3)}$) values for various materials.

Materials	Higher-order NLO susceptibility (χ ⁽³⁾) (esu)	Refs.
Orange CQDs	2.7742×10^{-7}	41
Cr:CdS QDs	0.7428×10^{-08}	42
Antimonene QDs	2.87×10^{-09}	43
CQD/GO SiO ₂	1.63×10^{-11}	44
N-CDs	$12.5 imes 10^{-12}$	45
carbon dots (CDs)	$11.3 imes 10^{-13}$	46
Manihot esculenta CQDs	5.5×10^{-6} (esu)	Present work

pathogens were sub-cultured in nutritional broth for 24 h at 37 °C. Around, 20 mL of germ free Muller-Hinton agar was loaded into culture petri dishes. The medium containing 10 μ g/mL of carbon quantum dots was loaded as well and incubated at 37 °C for 24 h the zone of inhibition (mm) is displayed in Fig. 8. The most notable finding of carbon quantum dots is a 43 mm inhibitory zone against gram-negative organisms *E. coli*.

Fig. 9 illustrates that CODs restrict the activity of antimicrobial agents. Growth inhibition can be described as membrane lysis caused by the interaction of positive charges on CD surfaces with negative charges on bacterial cell membranes. This adhesion causes physical and mechanical breakdown of the bacterial barrier, allowing CDs to penetrate the interior membranes. The membranes gradually collapse owing to a lack of electrolytes and cytoplasmic fluids [47-50]. Furthermore, the literature analysis indicates that amine groups on the surface of CDs denature DNA, resulting in cell death [51,52]. The antimicrobial assay is considered high (if the diameter of the inhibition region is >6 mm). So far, if the diameter of the ZOI is less than <6 mm, the activity is low [53]. Shahshahanipour et al. [54] has stated that the antibacterial tests of CDs led to intriguing findings indicating that Henna as raw materials. Therefore, the synthesized CDs destroy Gram +Ve and Gram -Ve antimicrobial agents [54]. Mahat et al. [55] has investigated the modified membrane of CQDs-PSF that can effectively perform as an antimicrobial against E. Coli gram +Ve bacteria, thereby improving the anti-fouling efficiency of the forward osmosis membrane [55]. Zhao et al. [56] has reported two multifunctional CDs that demonstrated superior bioactivity and function as possible non-toxic agents for fluorescence imaging of microbial species [56]. Marković et al. [57] explored how the structural and morphological characteristics of height-controlled quantum

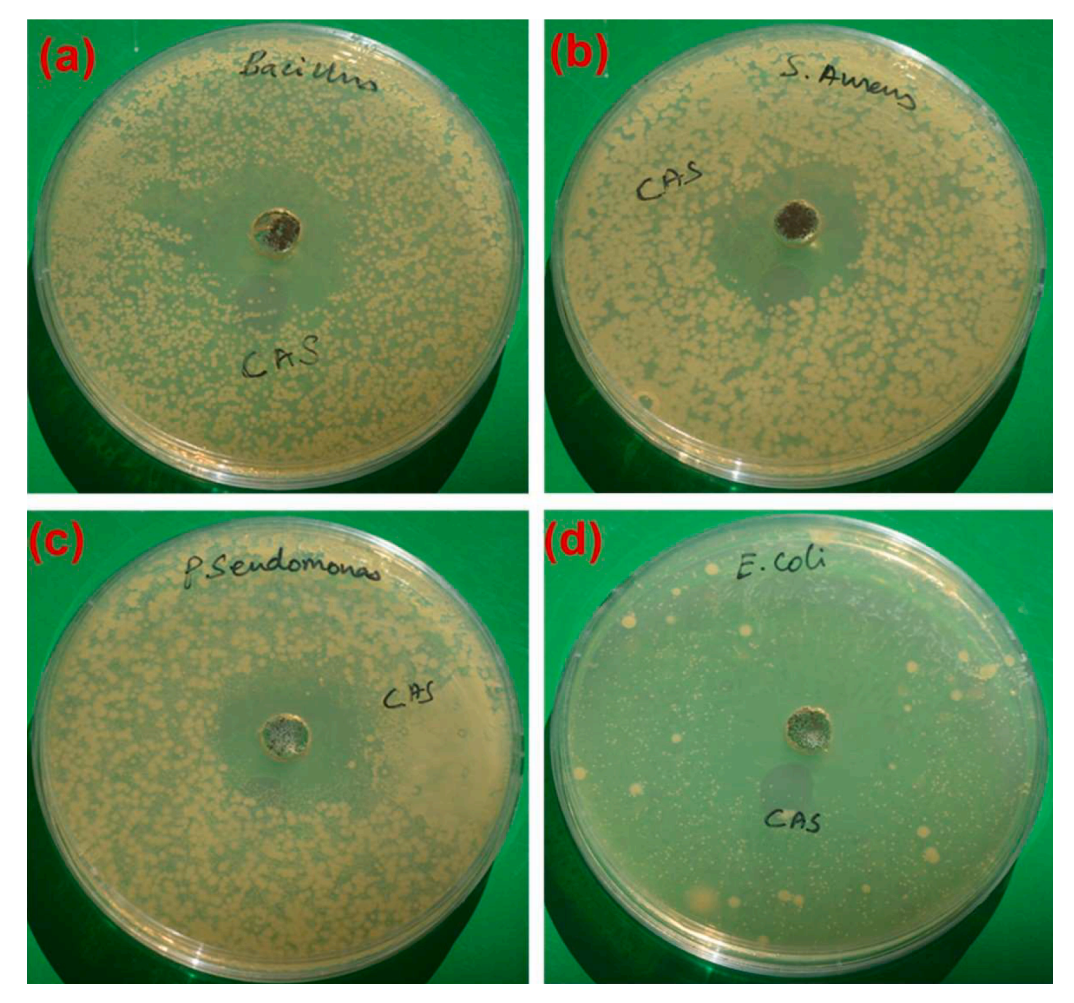


Fig. 8. Antibacterial activity plate photos of CQDs: (a) B. cereus (b) P. aeruginosa (c) S. aureus and (d) E. coli.

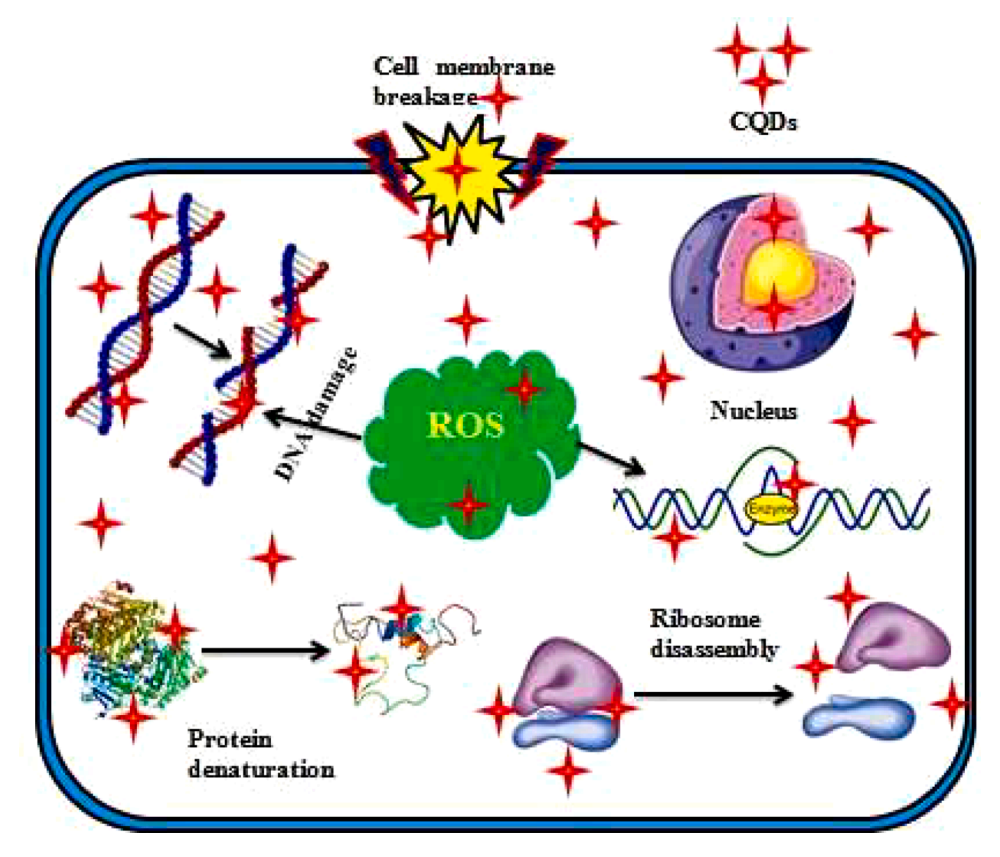


Fig. 9. Schematic mechanism diagram of antibacterial activity.

dots/polydimethylsiloxane (hCQDs/PDMS) influenced antimicrobial activity function [57]. Interestingly, in the current investigation, the CQDs exhibit greater inhibition against *B. cereus, S. aureus, P. aeruginosa*, and *E. coli*, and their antibacterial activity is compared to that of other CQDs (Table 3) [58–64]. As a result, the synthetic CQDs are suitable for medicinal applications.

4. Conclusion

In summary, CQDs were synthesized by simple hydrothermal method. It was then investigated by PXRD, FTIR, and XPS techniques, which confirmed the formation of CQDs and determined their size using HRTEM analysis to be 6.9 \pm 0.5 nm. The obtained CQDs in aqueous solution exhibited a sky blue color when exposed to UV light, and fluorescence experiments demonstrated their excitation-dependent fluorescence emission nature. White light emission of the material has been confirmed using CIE chromatic coordinate values. Z-scan results indicate that the synthesized CQDs exhibit significant optical nonlinearity and also satisfy the optical switching condition ($W>1,\ (T<1)$ representing that CQDs can be a good material for optical switching applications. CQDs with significant antibacterial activity have a high potential for bacterial infection resistance. This work also gives a prospective strategy for the development of CQDs-based photonic devices and biomedical applications.

CRediT authorship contribution statement

P. Surendran: Conceptualization, Methodology, Validation, Writing – original draft. A. Lakshmanan: Data curation, Validation, Visualization. S. Sakthy Priya: Investigation, Resources, Writing – review & editing. K. Balakrishnan: Resources, Writing – review & editing. P. Rameshkumar: Supervision, Writing – review & editing. Karthik Kannan: Writing – review & editing. K. Mahalakshmi: Visualization.

Table 3 shows a comparison of antibacterial activity for various quantum dots

Bacterial species	Samples	Zone of inhibition (mm)	Refs.
B. cereus	ZnS QDs	3.1	[58]
	Sugarcane CQDs	30	[59]
	Manihot esculenta	33	Present
	CQDs		work
S. aureus	Curcumin QDs	14	[60]
	Ananas comosus CQDs	25	[61]
	Nonylphenol CQDs	13	[62]
	Manihot esculenta	23	Present
	CQDs		work
P. aeruginosa	Curcumin CQDs	13	[60]
	Nonylphenol CQDs	11	[62]
	Sugarcane CQDs	24	[59]
	Manihot esculenta	30	Present
	CQDs		work
E. coli	Ananas comosus CQDs	39	[61]
	Cu QDs	11	[63]
	Tetracycline	19	[64]
	Manihot esculenta	43	Present
	CQDs		work

V. Gayathri: Data curation. G. Vinitha: Writing – review & editing.

Declaration of competing interest

The authors declare that they have no known competing financial interests or personal relationships that could have appeared to influence the work reported in this paper.

Data availability

Data will be made available on request.

Acknowledgements

P. S is grateful to the National Fellowship for Higher Education [F1-17.1/2015-16/NFST-2015-17-ST-TAM-1335], University Grant Commission, Government of India for financial support, and A. L would like to acknowledge the UGC-RGNF [F1-17.1/2016-17/RGNF-2015-17SC-TAM-21802], Government of India for the financial support.

References

- B.P. de Oliveira, F.O.M. da Silva Abreu, Carbon quantum dots synthesis from waste and by-products: perspectives and challenges, Mater. Lett. 282 (2021) 128764, https://doi.org/10.1016/j.matlet.2020.128764.
- [2] D. Ghosh, K. Sarkar, P. Devi, K.H. Kim, P. Kumar, Current and future perspectives of carbon and graphene quantum dots: from synthesis to strategy for building optoelectronic and energy devices, Renew. Sustain. Energy Rev. 135 (2021) 110391, https://doi.org/10.1016/j.rser.2020.110391.
- [3] A. Xu, G. Wang, Y. Li, H. Dong, S. Yang, P. He, G. Ding, Carbon-based quantum dots with solid-state photoluminescent: mechanism, implementation, and application, Small 16 (2020) 2004621, https://doi.org/10.1002/smll.202004621.
- [4] M. Gagic, S. Kociova, K. Smerkova, H. Michalkova, M. Setka, P. Svec, J. Pribyl, J. Masilko, R. Balkova, Z. Heger, L. Richtera, V. Adam, V. Milosavljevic, One-pot synthesis of natural amine-modified biocompatible carbon quantum dots with antibacterial activity, J. Colloid Interface Sci. 580 (2020) 30–48, https://doi.org/ 10.1016/j.icis.2020.06.125.
- [5] H.B. Ahmed, M.M. Mikhail, A.E.M. Abdallah, M. El-Shahat, H.E. Emam, Pyrimidine-5-carbonitrile derivatives as sprout for CQDs proveniences: antitumor and anti-inflammatory potentiality, Bioorg. Chem. 141 (2023) 106902, https://doi. org/10.1016/j.bioorg.2023.106902.
- [6] H.E. Emam, Clustering of photoluminescent carbon quantum dots using biopolymers for biomedical applications, Biocatal. Agric. Biotechnol. 42 (2022) 102382, https://doi.org/10.1016/j.bcab.2022.102382.
- [7] L.A. Adams, Tunable carbon quantum dots from starch via microwave assisted carbonization, Exp. Theor. Nanotechnol. 10 (2017) 13–21, https://doi.org/ 10.56053/1.1.13.
- [8] S. Wang, Z. Ma, T. Zhang, M. Bao, H. Su, Optimization and modeling of biohydrogen production by mixed bacterial cultures from raw cassava starch, Front. Chem. Sci. Eng. 11 (2017) 100–106, https://doi.org/10.1007/s11705-017-1617.3
- [9] M.Y. Pudza, Z.Z. Abidin, S. Abdul-Rashid, F.M. Yassin, A.S.M. Noor, M. Abdullah, Synthesis and characterization of fluorescent carbon dots from tapioca, ChemistrySelect 4 (2019) 4140–4146, https://doi.org/10.1002/slct.201900836.
- [10] S.P. Reddy Mallem, K.S. Im, J.H. Lee, C. Park, P. Bathalavaram, Trichromophore-doped cassava-based biopolymer as low-cost and eco-friendly luminous material for bio hybrid white-light-emitting diodes by dual-FRET process, Opt. Mater. 95 (2019) 109270, https://doi.org/10.1016/j.optmat.2019.109270 (Amst).
- [11] A.M. Nima, P. Amritha, V. Lalan, G. Subodh, Green synthesis of blue-fluorescent carbon nanospheres from the pith of tapioca (*Manihot esculenta*) stem for Fe(III) detection, J. Mater. Sci. Mater. Electron. 31 (2020) 21767–21778, https://doi.org/ 10.1007/s10854-020-04689-6.
- [12] A. Basu, A. Suryawanshi, B. Kumawat, A. Dandia, D. Guin, S.B. Ogale, Starch (Tapioca) to carbon dots: an efficient green approach to an on-off-on photoluminescence probe for fluoride ion sensing, Analyst 140 (2015) 1837–1841, https://doi.org/10.1039/C4AN02340D.
- [13] M. Yahaya Pudza, Z. Zainal Abidin, S. Abdul Rashid, F. Md Yasin, A.S.M. Noor, M. A. Issa, Eco-friendly sustainable fluorescent carbon dots for the adsorption of heavy metal ions in aqueous environment, Nanomaterials 10 (2020) 315, https://doi.org/10.3390/nano10020315.
- [14] S. Zhu, Q. Meng, L. Wang, J. Zhang, Y. Song, H. Jin, K. Zhang, H. Sun, H. Wang, B. Yang, Highly photoluminescent carbon dots for multicolor patterning, sensors, and bioimaging, Angew. Chem. Int. Ed. 52 (2013) 3953–3957, https://doi.org/ 10.1002/anie.201300519.
- [15] A. Tadesse, M. Hagos, D. RamaDevi, K. Basavaiah, N. Belachew, Fluorescentnitrogen-doped carbon quantum dots derived from citrus lemon juice: green synthesis, mercury (II) ion sensing, and live cell imaging, ACS Omega 5 (2020) 3889–3898, https://doi.org/10.1021/acsomega.9b03175.
- [16] Y. Wang, S. Kim, L. Feng, Highly luminescent N, S- Co-doped carbon dots and their direct use as mercury (II) sensor, Anal. Chim. Acta 890 (2015) 134–142, https://doi.org/10.1016/j.aca.2015.07.051.
- [17] H. Kaur, N. Kaur, N. Singh, Nitrogen and sulfur co-doped fluorescent carbon dots for the trapping of Hg (II) ions from water, Mater. Adv. 1 (2020) 3009–3021, https://doi.org/10.1039/D0MA00448K.
- [18] H.B. Ahmed, M. El-Shahat, A.K. Allayeh, H.E. Emam, Maillard reaction for nucleation of polymer quantum dots from chitosan-glucose conjugate: antagonistic for cancer and viral diseases, Int. J. Biol. Macromol. 224 (2023) 858–870, https:// doi.org/10.1016/j.iibiomac.2022.10.172.
- [19] H.B. Ahmed, H.E. Emam, Environmentally exploitable biocide/fluorescent metal marker carbon quantum dots, RSC Adv. 10 (2020) 42916–42929, https://doi.org/ 10.1039/d0ra06383e.
- [20] H.E. Emam, Carbon quantum dots derived from polysaccharides: chemistry and potential applications, Carbohydr. Polym. 324 (2024) 121503, https://doi.org/ 10.1016/j.carbpol.2023.121503.

- [21] H.E. Emam, M. El-Shahat, A.K. Allayeh, H.B. Ahmed, Functionalized starch for formulation of graphitic carbon nanodots as viricidal/anticancer laborers, Biocatal. Agric. Biotechnol. 47 (2023) 102577, https://doi.org/10.1016/j. beab 2022 102577
- [22] I.S. Marae, W. Sharmoukh, E.A. Bakhite, O.S. Moustafa, M.S. Abbady, H.E. Emam, Durable fluorescent cotton textile by immobilization of unique tetrahydrothienoisoquinoline derivatives, Cellulose 28 (2021) 5937–5956, https://doi.org/10.1007/s10570-021-03871-1.
- [23] O.L. Ugorji, O.N.C. Umeh, C.O. Agubata, D. Adah, N.C. Obitte, A. Chukwu, The effect of noisome preparation methods in encapsulating 5-fluorouracil and real time cell assay against HCT-116 colon cancer cell line, Heliyon 8 (2022) e12369, https://doi.org/10.1016/j.heliyon.2022.e12369.
- [24] H. Lin, L. Ding, B. Zhang, J. Huang, Detection of nitrite based on fluorescent carbon dots by the hydrothermal method with folic acid, R. Soc. Open Sci. 5 (2018) 172149, https://doi.org/10.1098/rsos.172149.
- [25] A. Kumar, A.R. Chowdhuri, D. Laha, T.K. Mahto, P. Karmakar, S.K. Sahu, Green synthesis of carbon dots from Ocimum sanctum for effective fluorescent sensing of Pb²⁺ ions and live cell imaging, Sens. Actuators B Chem. 242 (2017) 679–686, https://doi.org/10.1016/j.snb.2016.11.109.
- [26] R. Yang, X. Guo, L. Jia, Y. Zhang, Z. Zhao, F. Lonshakov, Green preparation of carbon dots with mangosteen pulp for the selective detection of Fe³⁺ ions and cell imaging, Appl. Surf. Sci. 423 (2017) 426–432, https://doi.org/10.1016/j. apsusc.2017.05.252.
- [27] G. Gedda, C.Y. Lee, Y.C. Lin, H. Wu, Green synthesis of carbon dots from prawn shells for highly selective and sensitive detection of copper ions, Sens. Actuators B Chem. 224 (2016) 396–403, https://doi.org/10.1016/j.snb.2015.09.065.
- [28] M. Fan, Z. Wang, K. Sun, A. Wang, Y. Zhao, Q. Yuan, R. Wang, J. Raj, J. Wu, J. Jiang, L. Wang, N-B-OH site-activated graphene quantum dots for boosting electrochemical hydrogen peroxide production, Adv. Mater. 35 (2023), https://doi.org/10.1002/adma.202209086.
- [29] H. Guo, X. Zhang, Z. Chen, L. Zhang, L. Wang, J. Xu, M. Wu, High-energy short-wave blue light conversion films via carbon quantum dots for preventing retinal photochemical damage, Carbon 199 (2022) 431–438, https://doi.org/10.1016/j.carbon.2022.08.003.
- [30] W. Hou, H. Guo, M. Wu, L. Wang, Amide covalent bonding engineering in heterojunction for efficient solar-driven CO 2 reduction, ACS Nano 17 (2023) 20560–20569, https://doi.org/10.1021/acsnano.3c07411.
- [31] X. Zhang, H. Guo, C. Chen, B. Quan, Z. Zeng, J. Xu, Z. Chen, L. Wang, Tunable photoacoustic and fluorescence imaging of nitrogen-doped carbon quantum dots, Appl. Mater. Today 30 (2023) 101706, https://doi.org/10.1016/j.
- [32] S. Rajapandi, M. Pandeeswaran, G.N. Kousalya, Novel green synthesis of N-doped carbon dots from fruits of Opuntia ficus Indica as an effective catalyst for the photocatalytic degradation of methyl orange dye and antibacterial studies, Inorg. Chem. Commun. 146 (2022) 110041, https://doi.org/10.1016/j. inoche.2022.110041.
- [33] K. Senthil, S. Kalainathan, A.R. Kumar, P.G. Aravindan, Investigation of synthesis, crystal structure and third-order NLO properties of a new stilbazolium derivative crystal: a promising material for nonlinear optical devices, RSC Adv. 4 (2014) 56112–56127, https://doi.org/10.1039/C4RA09112D.
- [34] H. Li, Z. Kang, Y. Liu, S.T. Lee, Carbon nanodots: synthesis, properties and applications, J. Mater. Chem. 22 (2012) 24230, https://doi.org/10.1039/
- [35] P. Yu, X. Wen, Y.R. Toh, J. Tang, Temperature-dependent fluorescence in carbon dots, J. Phys. Chem. C 116 (2012) 25552–25557, https://doi.org/10.1021/ in3073087
- [36] L. Rao, Q. Zhang, M. Wen, Z. Mao, H. Wei, H.J. Chang, X. Niu, Solvent regulation synthesis of single-component white emission carbon quantum dots for white lightemitting diodes, Nanotechnol. Rev. 10 (2021) 465–477, https://doi.org/10.1515/ ntrev-2021-0036.
- [37] W. Zhou, Z. Sun, J. Fan, W. Huang, J. Zhang, H. Song, L. Zhou, J. Huang, Z. Wu, X. Zhang, Novel solution and solid-state emissive long-wavelength carbon dots for water sensing and white LED applications, Spectrochim. Acta Part A Mol. Biomol. Spectrosc. 304 (2024) 123328, https://doi.org/10.1016/j.saa.2023.123328.
- [38] X.Y. Zhang, M.P. Zhuo, L.S. Liao, Light-emitting carbon dots extracted from naturally grown torreya grandis seeds, Org. Electron. 96 (2021) 106255, https:// doi.org/10.1016/j.orgel.2021.106255.
- [39] M. Sheik-bahae, A.A. Said, E.W. Van Stryland, High-sensitivity, single-beam n₂ measurements, Opt. Lett. 14 (1989) 955, https://doi.org/10.1364/OL.14.000955.
- [40] S. Mathew, A.R. Chacko, B.K. Korah, M. Susan Punnose, B. Mathew, Green synthesized carbon quantum dot as dual sensor for Fe(II) ions and rational design of catalyst for visible light mediated abatement of pollutants, Appl. Surf. Sci. 606 (2022) 154975, https://doi.org/10.1016/j.apsusc.2022.154975.
- [41] P. Surendran, A. Lakshmanan, G. Vinitha, G. Ramalingam, P. Rameshkumar, Facile preparation of high fluorescent carbon quantum dots from orange waste peels for nonlinear optical applications, Luminescence 35 (2020) 196–202, https://doi.org/ 10.1002/bio.3713.
- [42] M. Khanzadeh, M. Dehghanipour, M. Karimipour, M. Molaei, Improvement of nonlinear optical properties of graphene oxide in mixed with Ag₂S@ZnS coreshells, Opt. Mater. 66 (2017) 664–670, https://doi.org/10.1016/j. optmat.2017.03.008 (Amst).
- [43] L. Lu, X. Tang, R. Cao, L. Wu, Z. Li, G. Jing, B. Dong, S. Lu, Y. Li, Y. Xiang, J. Li, D. Fan, H. Zhang, Broadband nonlinear optical response in few-layer antimonene and antimonene quantum dots: a promising optical Kerr media with enhanced stability, Adv. Opt. Mater. 5 (2017) 1700301, https://doi.org/10.1002/adom.201700301.

- [44] C. Zheng, L. Huang, Q. Guo, W. Chen, W. Li, Nonlinear optical responses of carbon quantum dots anchored on graphene oxide hybrid in solid-state transparent monolithic silica gel glasses, Opt. Laser Technol. 107 (2018) 281–290, https://doi. org/10.1016/j.optlastec.2018.06.013.
- [45] L. Bai, S. Qiao, H. Li, Y. Fang, Y. Yang, H. Huang, Y. Liu, Y. Song, Z. Kang, N-doped carbon dot with surface dominant non-linear optical properties, RSC Adv. 6 (2016) 95476–95482, https://doi.org/10.1039/c6ra18837k.
- [46] L. Ma, W. Xiang, H. Gao, J. Wang, Y. Ni, X. Liang, Facile synthesis of tunable fluorescent carbon dots and their third-order nonlinear optical properties, Dyes Pigments 128 (2016) 1–7, https://doi.org/10.1016/j.dyepig.2016.01.005.
- [47] K. Rajendiran, Z. Zhao, D.D. Pei, A. Fu, Antimicrobial activity and mechanism of functionalized quantum dots, Polymers 11 (2019) 1670, https://doi.org/10.3390/ polym11101670
- [48] M. Thakur, S. Pandey, A. Mewada, V. Patil, M. Khade, E. Goshi, M. Sharon, Antibiotic conjugated fluorescent carbon dots as a theranostic agent for controlled drug release, bioimaging, and enhanced antimicrobial activity, J. Drug Deliv. (2014) 1–9, https://doi.org/10.1155/2014/282193.
- [49] G. Gedda, S.A. Sankaranarayanan, C.L. Putta, K.K. Gudimella, A.K. Rengan, W. M. Girma, Green synthesis of multifunctional carbon dots from medicinal plant leaves for antimicrobial, antioxidant, and bioimaging applications, Sci. Rep 13 (2023) 6371, https://doi.org/10.1038/s41598-023-33652-8.
- [50] Y. Sun, M. Zhang, B. Bhandari, C. Yang, Recent development of carbon quantum dots: biological toxicity, antibacterial properties and application in foods, Food Rev. Int. (2020), https://doi.org/10.1080/87559129.2020.1818255.
- [51] N. Tejwan, M. Kundu, N. Ghosh, S. Chatterjee, A. Sharma, T. Abhishek Singh, J. Das, P.C. Sil, Synthesis of green carbon dots as bioimaging agent and drug delivery system for enhanced antioxidant and antibacterial efficacy, Inorg. Chem. Commun. 139 (2022) 109317, https://doi.org/10.1016/j.inoche.2022.109317.
- [52] Q. Li, X. Shen, D. Xing, Carbon quantum dots as ROS-generator and scavenger: a comprehensive review, Dyes Pigments 208 (2022) 110784, https://doi.org/ 10.1016/j.dvepig.2022.110784.
- [53] M.J. Hajipour, K.M. Fromm, A. Akbar Ashkarran, D. Jimenez de Aberasturi, I.R. de Larramendi, T. Rojo, V. Serpooshan, W.J. Parak, M. Mahmoudi, Antibacterial properties of nanoparticles, Trends Biotechnol. 30 (2012) 499–511, https://doi. org/10.1016/j.tibtech.2012.06.004.
- [54] M. Shahshahanipour, B. Rezaei, A.A. Ensafi, Z. Etemadifar, An ancient plant for the synthesis of a novel carbon dot and its applications as an antibacterial agent and probe for sensing of an anti-cancer drug, Mater. Sci. Eng. C 98 (2019) 826–833, https://doi.org/10.1016/j.msec.2019.01.041.
- [55] N.A. Mahat, S.A. Shamsudin, N. Jullok, A.H. Ma'Radzi, Carbon quantum dots embedded polysulfone membranes for antibacterial performance in the process of

- forward osmosis, Desalination 493 (2020) 114618, https://doi.org/10.1016/j.desal.2020.114618.
- [56] D. Zhao, X. Liu, R. Zhang, X. Xiao, J. Li, Preparation of two types of silver-doped fluorescent carbon dots and determination of their antibacterial properties, J. Inorg. Biochem. 214 (2021) 111306, https://doi.org/10.1016/j. jinorgbio.2020.111306.
- [57] Z.M. Marković, M. Kováčová, P. Humpolíček, M.D. Budimir, J. Vajďák, P. Kubát, M. Mičušík, H. Švajdlenková, M. Danko, Z. Capáková, M. Lehocký, B.M. Todorović Marković, Z. Špitalský, Antibacterial photodynamic activity of carbon quantum dots/polydimethylsiloxane nanocomposites against Staphylococcus aureus, Escherichia coli and Klebsiella pneumoniae, Photodiagn. Photodyn. Ther. 26 (2019) 342–349, https://doi.org/10.1016/j.pdpdt.2019.04.019.
- [58] J.M. Baruah, S. Kalita, J. Narayan, Green chemistry synthesis of biocompatible ZnS quantum dots (QDs): their application as potential thin films and antibacterial agent, Int. Nano Lett. 9 (2019) 149–159, https://doi.org/10.1007/s40089-019-0270-x
- [59] S. Pandiyan, L. Arumugam, S.P. Srirengan, R. Pitchan, P. Sevugan, K. Kannan, G. Pitchan, T.A. Hegde, V. Gandhirajan, Biocompatible carbon quantum dots derived from sugarcane industrial wastes for effective nonlinear optical behavior and antimicrobial activity applications, ACS Omega 5 (2020) 30363–30372, https://doi.org/10.1021/acsomega.0c03290.
- [60] B. De, N.A. Karak, Green and facile approach for the synthesis of water soluble fluorescent carbon dots from banana juice, RSC Adv. 3 (2013) 8286–8290, https://doi.org/10.1039/c3ra00088e.
- [61] P. Surendran, A. Lakshmanan, S. Sakthy Priya, P. Geetha, P. Rameshkumar, K. Kannan, T.A. Hegde, G. Vinitha, Fluorescent carbon quantum dots from Ananas comosus waste peels: a promising material for NLO behaviour, antibacterial, and antioxidant activities, Inorg. Chem. Commun. 124 (2021) 108397, https://doi.org/ 10.1016/j.inoche.2020.108397.
- [62] S. Singh, P. Nigam, A. Pednekar, S. Mukherjee, A. Mishra, Carbon quantum dots functionalized agarose gel matrix for in solution detection of nonylphenol, Environ. Technol. 41 (2020) 322–328, https://doi.org/10.1080/09593330.2018.1498133.
- [63] S. Sheik Mydeen, R.R. Kumar, M. Kottaisamy, V.S. Vasantha, Biosynthesis of ZnO nanoparticles through extract from prosopis juliflora plant leaf: antibacterial activities and a new approach by rust-induced photocatalysis, J. Saudi Chem. Soc. 24 (2020) 393-406, https://doi.org/10.1016/j.jscs.2020.03.003.
- [64] M. Alavi, N. Karimi, Biosynthesis of Ag and Cu NPs by secondary metabolites of usnic acid and thymol with biological macromolecules aggregation and antibacterial activities against multi drug resistant (MDR) bacteria, Int. J. Biol. Macromol. 128 (2019) 893–901, https://doi.org/10.1016/j.ijbiomac.2019.01.177.